Brownian Molecular Dynamics Simulation on Self-Assembly Behavior of Diblock Copolymers: Influence of Chain Conformation

Shaoliang Lin,*,† Xiaohua He,‡ Yongliang Li,† Jiaping Lin,*,† and Takuhei Nose§

Key Laboratory for Ultrafine Materials of Ministry of Education, School of Materials Science and Engineering, East China University of Science and Technology, Shanghai 200237, China, Department of Chemistry, East China Normal University, Shanghai 200062, China, and Department of Nanochemistry, Tokyo Polytechnic University, Atsugi, Kanagawa 243-0297, Japan

Received: May 20, 2009; Revised Manuscript Received: September 4, 2009

Brownian molecular dynamic simulations are applied on the self-assembly behavior of AB-type diblock copolymers. The influence of chain conformation of core-forming A-block changing from rigid to flexible on the aggregation structure formed by AB copolymers is investigated. It is found that at a high rigid fraction f_R of A-block, a disk structure can be formed at a high aggregation interaction ε_{AA} of A-bead pairs because of the tendency of orientational packing of rigid portion within the aggregate core. Transitions of aggregation structure from disk to string, further to small aggregates, and to unimers are observed with decreasing ε_{AA}. The packing of A-blocks becomes more random at relatively lower values of f_R, resulting in the formation of spherical structure. The region of string becomes narrower while the regions of the small aggregates and sphere become wider as decreasing f_R. Meanwhile, the onsets of string, disk, and sphere formation move to higher ε_{AA}. The phase diagrams for the influences of rigid potion location within the A-block and the chain rigidity of the A-block are mapped. The comparison of simulation results with existing experimental observations is also presented. Our simulation results tend to bridge a gap of different micellization behaviors between rod−coil block copolymers and coil−coil block copolymers and extend to investigate chain conformation influence on phase diagram.

Introduction

The phase behavior and morphology of block copolymers consisting of coil−coil blocks or rod−coil blocks in solution as well as in melt have received much attention in both experimental[1−12] and theoretical viewpoints.[13−20] For the amphiphilic coil−coil diblock copolymers, many aggregation structures are observed in solution, such as sphere, cylinder, vesicle, and tubule. The self-assembly process of such blocks is mainly driven by an unfavorable mixing enthalpy and a small mixing entropy. However, for the rod−coil block copolymer, the difference in chain rigidity between rod and coil blocks is expected to greatly affect the self-assembly behavior because of the tendency of orientational packing of the rigid segments, which thus affects the nature of thermodynamically stable supramolecular structures.

Jenekhe and Chen studied the self-assembled aggregates of poly(phenylquinoline)-*b*-polystyrene rod−coil block copolymers in solution.[1,2] The morphologies of hollow spherical, vesicular, cylindrical, and lamellar aggregates were observed by changing the solvent composition. Kallitsis et al. reported that poly(2-hydroxyethyl methacrylate)-*b*-polystyrene rod−coil copolymers can form island, stringlike, and honeycomb-like structures.[7] These rod−coil molecular architectures impart the rod blocks into ordered structures because of the large difference in stiffness between rod and coil blocks. Unfortunately, all of these rigid segments have only restricted conformational freedom, and thus retain their rodlike character under virtually all circumstances. It is interesting to manipulate the aggregation structures of the diblock copolymers induced by the conformational changes.

There is limited work regarding the self-assembly behavior of block copolymers containing a chain conformation changeable molecule, such as polypeptide. It is well-known that polypeptide can take a high-order α-helix conformation as a rodlike segment in neutral solvent, which can be converted into a random coil conformation under certain conditions.[21−25] Babin et al. reported that polyisoprene-*b*-poly(L-lysine) copolymers in water can form a large micelle as the corona-forming poly(L-lysine) block taking a coil conformation. It was found that the aggregate size decreases as the polypeptide undergoes conformation transition into an α-helix.[26] Ding et al. studied the effect of chain conformation change on the self-assembly behavior of poly(γ-benzyl L-glutamate)-block-poly(ethylene glycol) (PBLG-*b*-PEG) in ethanol medium. They found that the conformation of the PBLG chain transforms from α-helix to random coil within the core, by introducing trifluoroacetic acid, which results in a change of the micelle structure from rod to sphere.[27]

Computer simulation has played an important role in investigating material properties and its physics.[28] Many simulation studies on the self-assembly behavior of amphiphilic coil−coil diblock copolymers were performed by applying various computational techniques such as Monte Carlo (MC),[29−33] molecular dynamics (MD),[34−39] and dissipative particle dynamics (DPD) simulations.[40−42] The self-assembly behavior of amphiphilic rod−coil copolymers by computer approaching was also reported.[43−46] Horsch et al. found that rodlike particles connected to a flexible tether at a concentrated concentration can self-assemble into spherical micelles with bcc order, long

* To whom correspondence should be addressed. Telephone: +86-21-6425-1011. Fax: +86-21-6425-3539. E-mail: linshaoliang@hotmail.com; jplinlab@online.sh.cn.
† East China University of Science and Technology.
‡ East China Normal University.
§ Tokyo Polytechnic University.

10.1021/jp904707a CCC: $40.75
Published on Web 09/29/2009

micelles with nematic order, a racemic mixture of hexagonally ordered chiral cylinders, and a smectic C lamellar phase.[44]

All of these copolymers applied in the computer simulation have only restricted conformation. There are few works reported on computer simulations for the effect of chain conformation on the phase-separation behavior. Cui et al. reported the aggregation of rod-flexible ABA and BAB triblock (A was rod block and repulsive with block B) copolymers in a thin film as a function of varying the rigidity of the rod block by MC simulation.[47] The ABA triblock copolymer film was likely to form a lamella structure with the increasing rigidity of block A, while the aggregation of BAB triblock copolymers tended to change from lamellar to cylinder structure with the increasing rigidity of block A. Song et al. studied the rigidity effect on phase behavior of symmetric ABA triblock copolymers containing a semiflexible midblock in melts by lattice MC simulation.[48] A lamellar structure was formed as the situation for fully flexible chains. It was revealed that the increase in midblock rigidity results in the increase in bridge chain fraction. However, no systematic work has been reported on computer simulation of micellization behavior of diblock copolymer containing a conformation changeable core-forming block thus far, to our knowledge. It is interesting to investigate the self-assembly behavior of such amphiphilic diblock copolymers with focused attention on influence of chain conformation transition, where the conformational rigidity of the insoluble block is varied along its chain.

In our previous work, we carried out Brownian dynamic simulations on the micellization behavior of amphiphilic rod−coil copolymers.[46] It was revealed that such copolymers in solution can form a novel twisted string in addition to a disk structure. Changes of chain length and segregation intensity of rod−rod pairs can change the aggregation structures and shift the phase diagrams. We will extend this rod−coil copolymer model to investigate the influence of chain conformation of rod−block (core-forming block) on the micellization behavior in solution in this work. The main purpose is to bridge a gap of different micellization behaviors between rod−coil copolymers and coil−coil copolymers.

In this work, we perform Brownian molecular dynamic simulations based on our previous model, on the self-assembly behavior of amphiphilic AB diblock copolymers. The influence of chain conformation of core-forming A-block changing from rigid (rod) to flexible (coil) on the aggregation structure is investigated. Structural transitions of aggregates are found as changing the chain rigid fraction of A-block and Lennard-Jones interaction of A-bead pairs. Diagrams for the regions of thermodynamic stability of disk, string, sphere, and small aggregates are constructed. The influences of rigid potion location within the A-block and the chain rigidity of the A-block on the self-assembly behavior are also presented. Some simulation results are compared with existing experimental observations.

Method of Simulation

The simulations are performed by using the simulator, coarse-grained molecular dynamics program (COGNAC) of OCTA. The simulator was developed by Doi's group, which is public on a Web site.[49] COGNAC uses the reduced unit system for setting data. To convert it to real units, a set of unit parameters is given in our previous article.[46]

Molecular Model and Simulation Conditions. To construct AB-type diblock copolymer molecules and their assembly, the potentials that should be given are the bonding potential, U_{mol}, and the nonbonding potential, U_{ij}. The former can construct a desired molecule from atoms, while the latter describes intermolecular interactions. An AB-type diblock copolymer molecule is represented by a linear chain consisting of several beads connected by a bond stretching potential $U_{bond}(r)$. In this work, an A-block with eight beads and a B-block with nine beads, coded as A_8B_9, are constructed. An illustration of this copolymer molecule model is shown in Figure 1. The blue beads are the hydrophobic A-block with variable chain conformation (i.e., rod or coil), and the green beads are the hydrophilic B-block with a flexible form. To realize an A-block with a rigid form, an angle bending potential $U_{angle}(\theta)$ is introduced. The B-block has no angle bending potential constraint and represents a flexible chain, as shown in Figure 1. Therefore, U_{mol} is a combination of $U_{bond}(r)$ and $U_{angle}(\theta)$. The setting values for $U_{bond}(r)$ are the same as those in ref 45.

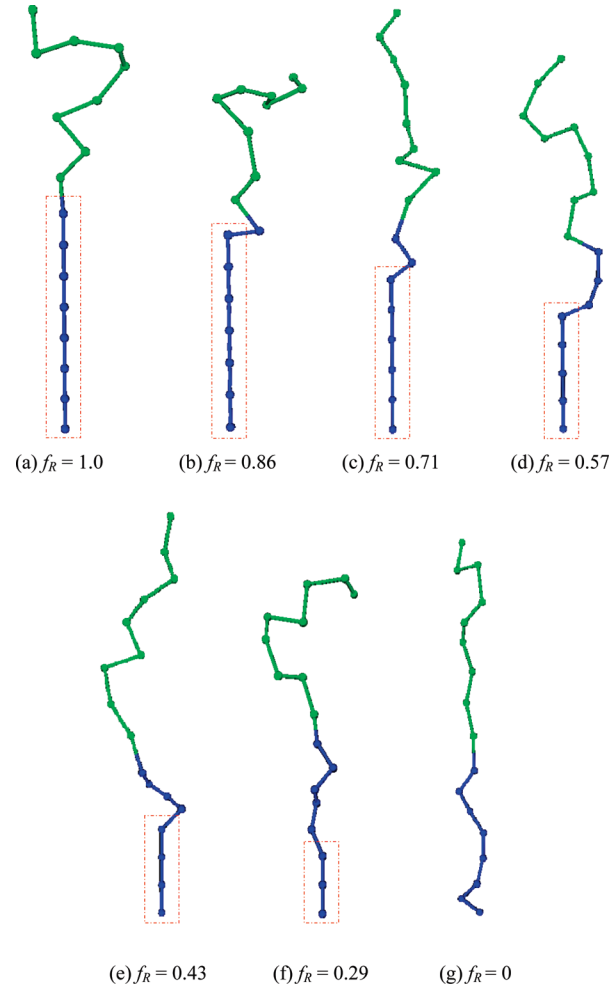

Figure 1. Layouts of A_8B_9 diblock copolymer with various rigid fraction f_R of the A8 block. The blue beads are the hydrophobic A-block and the green beads are hydrophilic B-block. The f_R values for the rigid portion within the A-block (shown in red rectangles) are presented below the copolymer schemes.

For the rigid A-block, the angle bending potential, $U_{angle}(\theta)$, is given by a cosine harmonic function of the angle θ defined by the three chemically connected beads.

$$U_{angle}(\theta) = \frac{1}{2}k_a(\cos\theta - \cos\theta_0)^2 \quad (1)$$

where k_a is the angle spring constant, and θ_0 is the equilibrium angle. The larger the value of k_a, the more rigid the molecule

chain.[50] To realize an A-block with a rigid form, the equilibrium angle θ_0 is set to a value of 0.1° (essentially zero). The magnitude of the constant k_a is set to be 10 000 in most cases.

The interaction energy U_{ij} is given by the standard Lennard-Jones 12:6 potential U_{ij} acting between any pair of beads i and j:

$$U_{ij} = \begin{cases} 4\varepsilon_{ij}\left[\left(\frac{\sigma_{ij}}{r_{ij}}\right)^{12} - \left(\frac{\sigma_{ij}}{r_{ij}}\right)^{6} - \left(\frac{\sigma_{ij}}{r_{ij}^{c}}\right)^{12} + \left(\frac{\sigma_{ij}}{r_{ij}^{c}}\right)^{6}\right], & r \le r_{ij}^{c} \\ 0, & r > r_{ij}^{c} \end{cases} \quad (2)$$

where r_{ij}^{c} is the cutoff distance, $r_{ij} = |\vec{r}_i - \vec{r}_j|$, with $\vec{r}_i$ and $\vec{r}_j$ being the locations of the i-th and j-th beads, respectively. The amphiphilicity in this model is realized using a method mentioned by Bourov and Bhattacharya.[51,52] They introduced an attractive cutoff for the A−A interaction ($r_{AA}^{c} = 2.5$) and a repulsive cutoff distance for the A−B and B−B interactions ($r_{AB}^{c} = 2^{1/6}$, $r_{BB}^{c} = 2^{1/6}$). Such selections of r_{ij}^{c} drive the A-blocks to form the core of micelles. The diameter σ of an LJ bead is kept at unity for any pairs of species. The pairwise interaction ε_{AA} between A-beads is chosen to be variable, while the other interactions are all set to be unity (i.e., $\varepsilon_{AB} = \varepsilon_{BB} = 1.0$).

In this work, we focus on the influence of the chain conformation of the A-block on the self-assembly behavior of AB copolymers. The AB copolymers with various chain conformations of the A-block, changing from rigid to flexible, are illustrated in Figure 1. The fractions (f_R) of the rigid conformation of A-blocks are also presented, which is realized by the angle bending potential. Here f_R is given by $(n - 1)/(m - 1)$, where n is the number of beads in the rigid form within the A-block (shown in red rectangles in Figure 1) and m is the total number of the beads of the A-block.

All the simulations were carried out on a cubic cell ($60 \times 60 \times 60$) using a dynamic algorithm with temperature controlling method (NVT ensemble). The Brownian dynamics, developed by Grest and Kremer,[53] was employed in this work. The effect of solvent molecules was implicitly treated by the noise term.[54] Periodic boundary conditions were imposed to minimize the effect of finite system size. A regular body-centered-cubic (BCC) packing lamellar mode for 100 A_8B_9 copolymers was applied to generate the initial structures of molecules, and the structure was relaxed by stochastic dynamic simulation using an integration time step $\Delta t = 0.004$. The lengths of simulation runs were 3×10^6 time steps (i.e., 12 000 time units), which ensured that the simulated system reached equilibrium. All calculations were performed at a temperature $T = 3.0$.

Results

In this section, only one type of copolymer with a fixed length of A_8B_9 is described. We present the results of the Brownian molecular dynamics simulation regarding the micellization behavior of AB block copolymers and the dependence of aggregation structures on chain conformation of the core-forming A-block.

Evolution of Micelle Structure with Changing Rigid Fraction of A-Block. To visualize changes in micelle structure and molecular packing with changing rigid fraction f_R as well as the aggregation strength ε_{AA} of A-blocks, typical snapshots of A_8B_9 copolymer systems with various simulation conditions are presented. Figure 2 illustrates the various micelle structures obtained with a fully rigid A-block (i.e., rigid fraction $f_R = 1.0$). Here the A-block is blue and the B-block is green. In the case of the stronger interaction of $\varepsilon_{AA} = 2.4$ (snapshot (i) in Figure 2a), the aggregated rod blocks tend to align in parallel in the core of the micelle. Snapshot (ii) in Figure 2a shows that the geometric structure of this micelle core is of a circlelike form viewed from the direction along the rod (A-block) alignment axis. A similar disk (disklike) micelle structure can be found at $\varepsilon_{AA} \ge 2.2$. At the intermediate segregation strengths ($1.8 \le \varepsilon_{AA} < 2.2$), a string (cylinder-like) structure is observed. A typical snapshot for $\varepsilon_{AA} = 2.0$ is shown in Figure 2b. Snapshot (i) illustrates an unusual molecule packing of A-blocks. In each section of the string micelle, the A-block tends to align along an orientation vector, and this vector gradually rotates along the long-center-axis of the string. That is, the micelle is a twisted string. With a further decrease in the segregation strength, the twisted string micelle is broken into small aggregates coexisting with some single copolymers (unimers), as can be seen in the snapshot of $\varepsilon_{AA} = 1.7$ in Figure 2c. We call these broken micelles "small aggregates". With a further decrease in ε_{AA}, more and more unimers come out of the small aggregates. When ε_{AA} is lower than a certain value (critical micelle interaction, CMI), no aggregates remain, and at $\varepsilon_{AA} < 1.6$, only free unimers are found, distributed randomly in the system (snapshot not included).

Figure 3 presents typical snapshots of the A_8B_9 copolymer system with $f_R = 0.71$. As can be seen in Figure 3a, the rigid portions of A-blocks align in parallel within the core, and a disk micelle is formed for values of $\varepsilon_{AA} \ge 2.3$. At the intermediate segregation strength $2.0 \le \varepsilon_{AA} < 2.3$, a long string micelle is observed (typical snapshots with $\varepsilon_{AA} = 2.1$ are shown in Figure 3b). However, the A-blocks pack with less order within the core as compared to Figure 2b with a fully rigid A-block, $f_R = 1.0$. Upon further decreasing ε_{AA}, the string is broken into small aggregates and dissociates into unimers.

Snapshots in Figure 4 illustrate the consequences of a further decrease of f_R to 0.43. A disklike structure can be seen in Figure 4a ($\varepsilon_{AA} = 3.0$), where rigid portions of A-blocks still tend to align in parallel and show some order within the core. With a decrease in ε_{AA} to 2.7, a spherical structure formed by the AB blocks can be observed, where the A-blocks pack randomly within the core surrounded by B blocks, as shown in Figure 4b.

A phase diagram of rigid fraction f_R of A-block versus segregation strength ε_{AA} for the solution of AB blocks is presented in Figure 5. This diagram illustrates the influence of chain conformation of the A-block, from rigid rod to flexible coil, on the self-assembly behavior. The regions of disk, string, sphere, small aggregates, and unimers are indicated. As can be seen from Figure 5, the AB copolymers form a disk micelle at high LJ interaction of ε_{AA} with high rigid fraction f_R of the A-block (for example, $f_R = 1.0$). A transition from disk to string micelle is found when ε_{AA} is decreased, and then the string micelle is broken into a small aggregates region. With a further decrease in ε_{AA}, the system transforms into unimers. Figure 5 also shows that with decreasing f_R to 0.57, the region of string micelles becomes narrower, while the region of small aggregates becomes wider. The onsets of string and disk formation move to higher ε_{AA}. With a further decrease in f_R, the region of string micelles disappears and a spherical micelle region appears. The region of spherical structures becomes wider, and the onset of such a structure moves to high ε_{AA}.

The influence of rigid fraction f_R of A-block on the CMI can also be observed in Figure 5. An increase of CMI with decreasing f_R is found. This result confirms that the driving

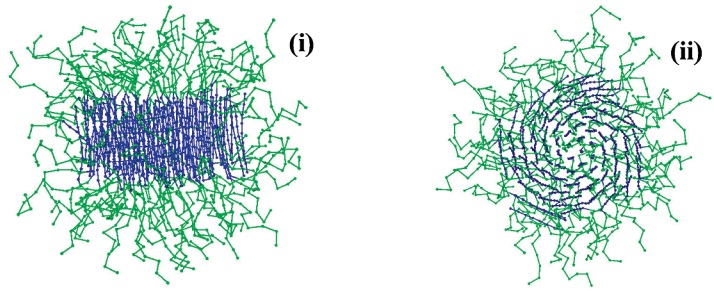

(a) ε_{AA} = 2.4 (i: side view perpendicular to the rigid portion axis; ii: top view along the rigid portion axis)

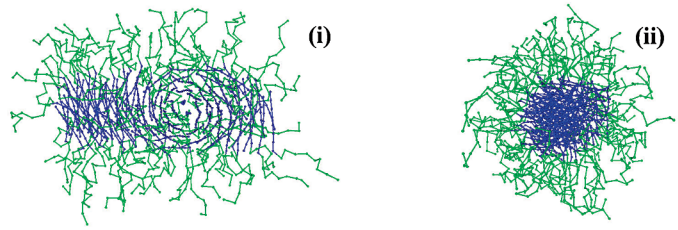

(b) ε_{AA} = 1.9 (i: top view perpendicular to the string axis; ii: side view along the string axis)

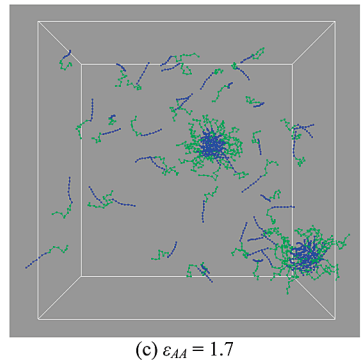

(c) ε_{AA} = 1.7

Figure 2. Snapshots of the A_8B_9 copolymer system with $f_R = 1.0$ at different ε_{AA} values: (a) $\varepsilon_{AA} = 2.4$, (b) $\varepsilon_{AA} = 1.9$, and (c) $\varepsilon_{AA} = 1.7$.

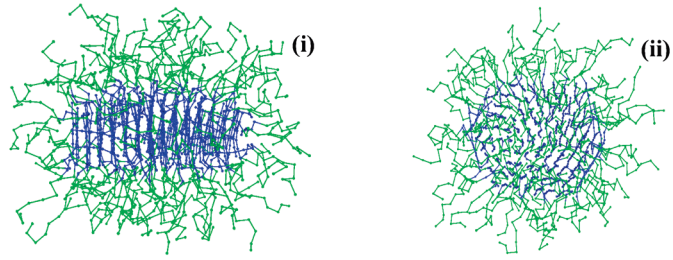

(a) ε_{AA} = 2.7 (i: side view perpendicular to the rigid portion axis; ii: top view along the rigid portion axis)

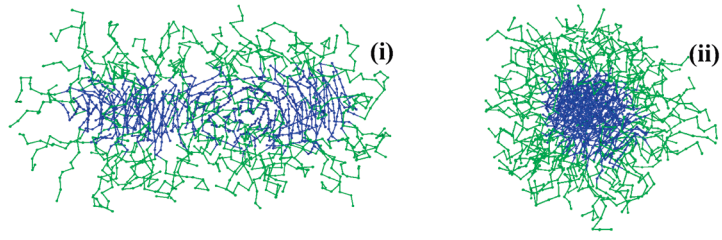

(b) ε_{AA} = 2.1 (i: top view perpendicular to the string axis; ii: side view along the string axis)

Figure 3. Snapshots of the A_8B_9 copolymer system with $f_R = 0.71$ at different ε_{AA} values: (a) $\varepsilon_{AA} = 2.7$ and (b) $\varepsilon_{AA} = 2.1$.

forces controlling the self-assembly formation of AB blocks containing rigid portions are expected to be primarily similar to flexible block copolymers.

In contrast to coil−coil diblock copolymers, the driving force for self-assembly of copolymers containing a rigid portion originates not only from the separation of rigid and flexible components, but also from the tendency of rodlike segments to form an ordered structure. Changing the rigid fraction of A-blocks and the aggregation intensity of A-block pairs affects the packing of A-blocks and can lead to various assembly

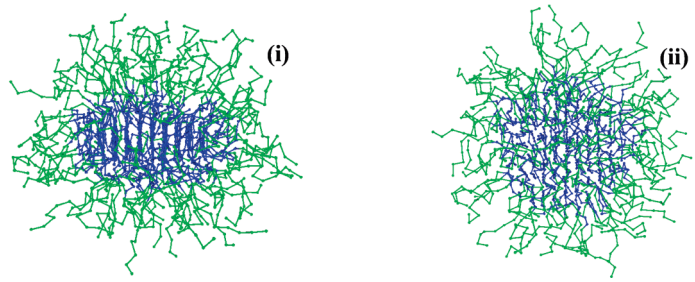

(a) ε_{AA} = 3.0 (i: side view perpendicular to the rigid portion axis; ii: top view along the rigid portion axis)

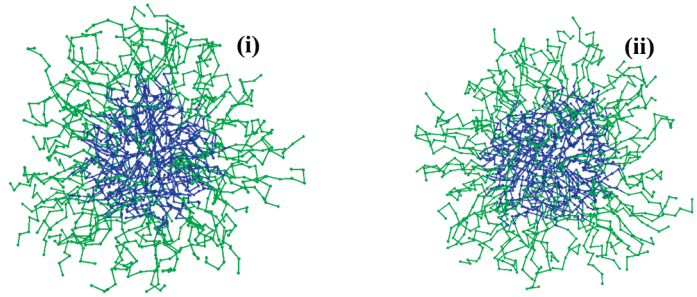

(b) ε_{AA} = 2.7 (i,ii: views from random directions)

Figure 4. Snapshots of A_8B_9 copolymer system with $f_R = 0.43$ at different ε_{AA} values: (a) $\varepsilon_{AA} = 3.0$ and (b) $\varepsilon_{AA} = 2.7$.

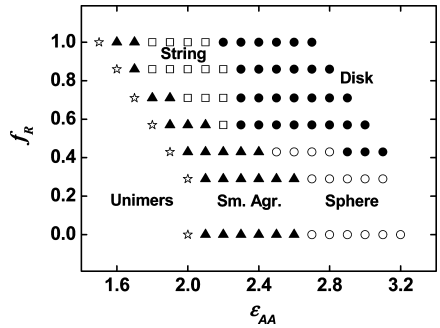

Figure 5. Simulation phase diagram for A_8B_9 diblock copolymers plotted in f_R vs ε_{AA}. Regions of disk (●), string (□), small aggregate (▲), sphere (○), and unimer (☆) are shown.

structures. Here we describe the alignment of the rigid portion of A-blocks within the core.[46] This alignment is characterized by the vector product, $u_i \cdot u_d$, of the normalized vector of the i-th rigid portion of the A-block, u_i, and the normalized vector of the orientation direction, u_d. The product represents the angle, ψ_i, between i-th rigid portion and the orientation direction of all of rigid portions, expressed as:

$$\cos(\psi_i) = u_i \cdot u_d \tag{3}$$

The alignment of rigid segments in the core can be described as a function of position of the rod block along the axis of the aggregation structure. Typical results for $\cos(\psi)$ for the alignment of rigid portions within the A-blocks are shown in Figure 6. As can be seen in Figure 6a for $\varepsilon_{AA} = 2.4$ and $f_R = 1.0$, most of the absolute values of $\cos(\psi)$ are close to 1.0, which suggests that the A-blocks align in parallel to each other to form a disklike structure as illustrated in Figure 2a. With the decrease in ε_{AA} to 1.9, illustrated in Figure 6b, the absolute values of $\cos(\psi)$ gradually change between 0 and 1.0 along the string axis. Such a periodic change of $\cos(\psi)$ indicates that the alignment of the rigid A-blocks twists as they pack to form the core of a string micelle. Hence, a twisted string is found. The example shown

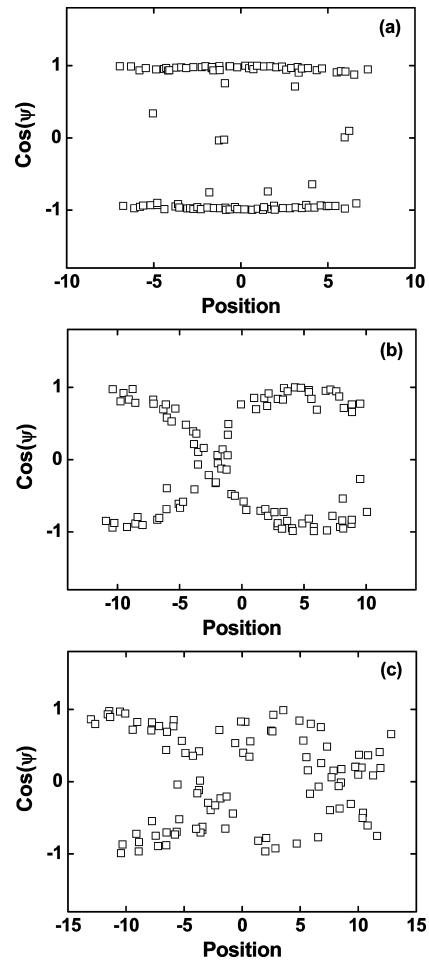

Figure 6. Vector product $\cos(\psi)$ for the rigid portion alignment of A-blocks as a function of position along the string axis: (a) $f_R = 1.0$, $\varepsilon_{AA} = 2.4$, (b) $f_R = 1.0$, $\varepsilon_{AA} = 1.9$, and (c) $f_R = 0.71$, $\varepsilon_{AA} = 2.0$.

in Figure 6c is for $f_R = 0.71$ and $\varepsilon_{AA} = 2.0$. The tendency of a gradual change of $\cos(\psi)$ and a more fluctuating value of $\cos(\psi)$

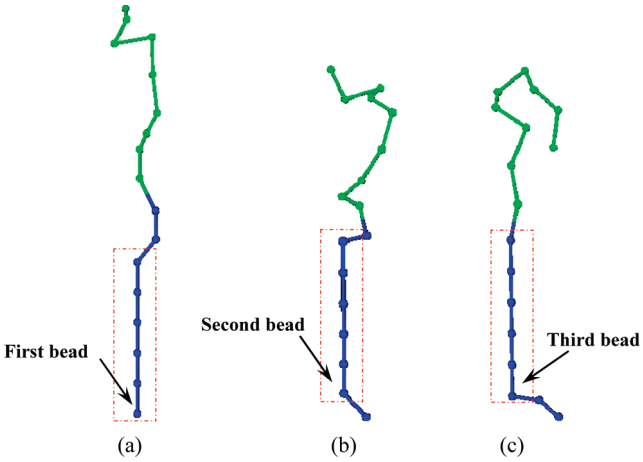

Figure 7. Layouts of A_8B_9 diblock copolymer at $f_R = 0.71$ with various rigid portion locations (shown in red rectangles) in A-block: (a) P1, (b) P2, and (c) P3.

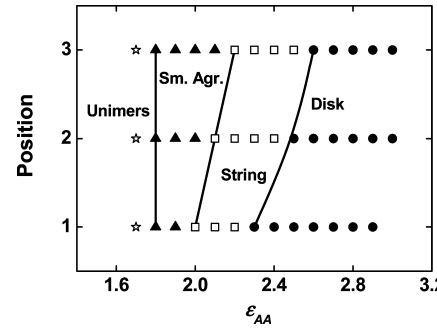

Figure 8. Simulation phase diagram for A_8B_9 diblock copolymers at $f_R = 0.71$ with various rigid portion locations in A-block. Regions of disk (●), string (□), small aggregate (▲), and unimer (☆) are shown.

can be found as compared to Figure 6b with a decreasing rigid fraction f_R. This result suggests that the rigid portions of A-blocks still tend to pack in a twisted alignment in the core of the string, but with a more random packing. Meanwhile, as can also be seen in Figure 6, the region of positions for $\cos(\psi)$ is enlarged from panel a to panel c in Figure 6, which suggests that the structure of micelle has changed with the variation in f_R and ε_{AA}.

Effect of Rigid Portion Location. On the basis of the Zimm−Bragg theory, the helix-to-coil transition of a polypeptide chain can take place at any position among the chain, where the rod portions are alternately joined by random coil portions.[23,24] The liquid crystalline phase behavior can be manipulated by the helix fraction. Even for a fixed rigid fraction, the difference in rigid portion locations can modify the phase behaviors.[24]

In this simulation, the influence of the rigid portion location within the A-blocks on the micellization behavior of AB diblock copolymers was also examined. Figure 7 illustrates the layouts of the A_8B_9 diblock copolymer at a fixed rigid fraction f_R of 0.71 with various rigid portion locations in the A-block. To make the rigid portion location clear, we define a location point as illustrated in the red scale in Figure 7. We define the bead, which is at the end of the AB block copolymer, in the A-block as the first bead. If this bead is one atom within the rigid conformation, we call it position one, coded as P1. If the first bead is flexible but the second bead is within the rigid conformation, we call it position two, coded as P2, and so on. For the A_8B_9 diblock copolymer with $f_R = 0.71$, there are three different locations of the rigid portion within the A-block, as illustrated in Figure 7. The effect of the rigid portion location on the phase behavior is shown in Figure 8. One can see that when the rigid portion in the A-block is close to the B-block, the regions of string and small aggregates become wider. Meanwhile, the onsets of string and disk formation move to higher ε_{AA}. Simultaneously no effect on the CMI can be found for the various locations of the rigid portion in the A-block.

We also examined the influence of various locations of rigid segments for lower values of f_R. Figure 9 illustrates the layouts of the A_8B_9 diblock copolymer at $f_R = 0.57$ with various rigid portion locations in the A-block. Four different cases are presented. The effect of the rigid portion location on the phase behavior for $f_R = 0.57$ is shown in Figure 10. As the rigid portion in A-block moves forward toward the B-block (from P1 to P2), the regions of string and small aggregates become wider. As the location of the rigid portion moves further to P3 and P4, the string aggregates disappear, and spherical aggregates appear. The onsets of string, sphere, and disk formation move to higher ε_{AA}. Meanwhile, no effect on the CMI can be detected

Effect of Chain Rigidity. As mentioned in Method of Simulation, the rigid portion of the A-block can be realized by combining the bond potential and an angle potential. The magnitude of the angle spring constant k_a can change the block conformation from rigid to flexible. The higher the k_a, the more rigid the A-block. Figure 11 shows the dependence of the end-to-end distance of the A-block on k_a. With increasing angle spring constant k_a, the end-to-end distance of A8 block initially increases and then tends to level off. This result suggests that larger k_a values induce greater rigidity of the A-block (i.e., the conformation of A-block changes from flexible to more rigid).

The influence of k_a on the self-assembly behavior of AB blocks was also examined. Figure 12 shows the phase diagram plotted as angle spring constant k_a vs ε_{AA}. Regions of disk, string, sphere, small aggregates, and unimers are found. As can be observed in Figure 12, AB block copolymers can form a disk micelle at high ε_{AA} with a high value of k_a (for example, $k_a =$ 10 000). A transition from disk to string micelle is found when ε_{AA} is decreased, and then the string micelle is broken into small aggregates. With a further decrease in ε_{AA}, the system evolves into a unimers region. As can be seen in Figure 12, with decreasing k_a (i.e., decreasing the chain rigidity of the A-block), the string region becomes narrower, while the region of small aggregates becomes wider. The onsets of string and disk formation move to higher ε_{AA}. At sufficient low values of k_a, where the A-block shows more flexibility, the string region disappears and spherical structures appear. Simultaneously, a slight increase of the CMI is found with decreasing k_a. Such a phase behavior induced by the decrease of k_a corresponds to that of decreasing the rigid fraction f_R of A-block as illustrated in Figure 5.

Discussion

Amphiphilic AB copolymers can form micelles with A-blocks as the hydrophobic inner core and B-blocks as the hydrophilic corona. Changes in the chain conformation of the A-block from rigid rod to flexible coil can affect the packing of A-blocks in the micelle core. The rigid portions of A-blocks tend to align as they pack in order to minimize the enthalpy, while the flexible portions favor randomly packing to maximize the entropy. The different packing manner of A-blocks with various chain conformations within the core can further affect the aggregation structure.

If the rigid portion of A-blocks is large enough, the rigidity of A-blocks may allow them to assemble with high orientational

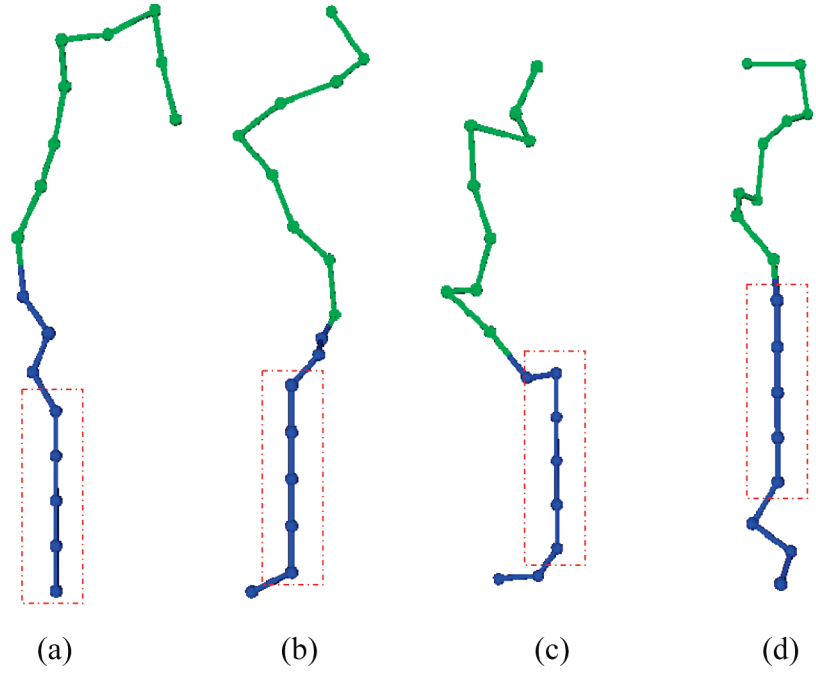

Figure 9. Layouts of A_8B_9 diblock copolymer at $f_R = 0.57$ with various rigid portion locations (shown in red rectangles) in A-block: (a) P1, (b) P2, (c) P3, and (d) P4.

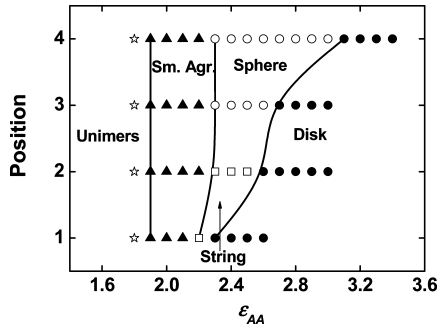

Figure 10. Simulation phase diagram for A_8B_9 diblock copolymers at $f_R = 0.57$ with various rigid portion locations in A-block. Regions of disk (●), string (□), small aggregate (▲), sphere (○), and unimer (☆) are shown.

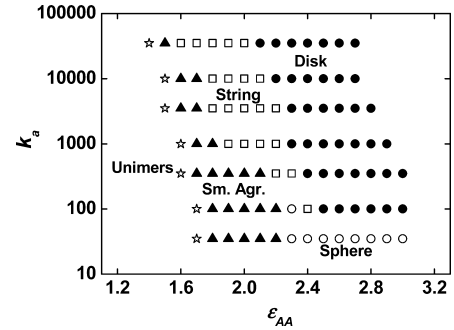

Figure 12. Simulation phase diagram for A_8B_9 diblock copolymers plotted in k_a vs ε_{AA}. Regions of disk (●), string (□), small aggregate (▲), sphere (○), and unimer (☆) are shown.

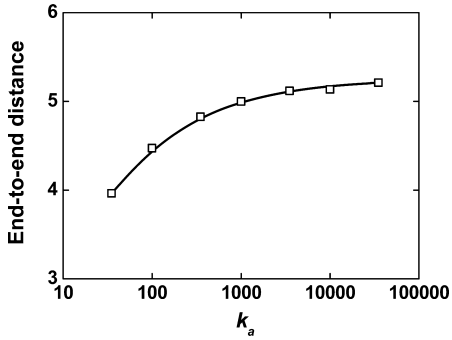

Figure 11. Dependence of end-to-end distance of A8 block on k_a.

order in the core. It is reasonable for A-blocks to align parallel to each other to form a disklike structure when the LJ interaction energy ε_{AA} of A-beads is high enough. However, such a structure induces a higher density of B-blocks in the micelle corona and at the A−B block interface. As ε_{AA} is decreased, the attraction of A-blocks is decreased. Meanwhile, the repulsion of B-blocks becomes dominant to relieve the coil stretching. Here a string micelle is formed because of the combination of enthalpic (or energetic) interaction of the A-blocks and the conformational entropy of the B-blocks and the flexible portions of the A-blocks. As ε_{AA} is further decreased, the attractive interaction of A-blocks does not have an enthalpy sufficient to form a long string, while the B-blocks want more space to explore. As a result, the string micelle is broken into small aggregates. The small aggregates break again, and only unassociated AB copolymers (unimers) exist in the system when the LJ interaction of A-bead pairs is sufficiently low.

The balance of the tendency for orderly packing of the rigid portions and random packing of the flexible portions of the A-blocks can result in various micelle structures. When the rigid conformation fraction of A-blocks is relatively low, the influence of flexible conformation within A-blocks becomes dominant, resulting in a more random packing of A-blocks within the core. Such a packing induces a spherical micelle structure, even at a high ε_{AA} of the A-beads. With decreasing ε_{AA}, the sphere breaks into small aggregates and finally into unimers. The different packing manner of A-blocks is the key to understanding the influence of the variation of the rigid fraction or chain rigidity on the micelle structure, as illustrated in Figures 5 and 12.

Some experimental evidence on the micellization behavior of block copolymers is available in the literature to support our simulation results. It is known that the spherical structures can be formed by coil−coil block copolymers in a selective

solvent.[8,9] Lamellar structures formed by rod−coil copolymers were also reported.[1,2] These morphologies formed by coil−coil copolymers and rod−coil copolymers coincide with our simulation results, where the spherical structure and disk structure can be formed by the A-block taking a flexible conformation or a rigid rod conformation, respectively. Ding et al. reported a variation in the structures formed by assembly of PBLG-*b*-PEG in ethanol.[27] A structural transition from rods into small spheres was induced by a conformation transition of the core-forming PBLG blocks from a helix to a random coil. This type of observation coincides with our simulation results as shown in Figure 5, where the aggregation structure is broken from string micelles into small aggregates with a decreasing rigid fraction of A-blocks.

Wang et al. prepared an aminoazobenzene-containing block copolymer PEO-*b*-PCN.[55] They reported that PEO-*b*-PCN can form uniform spherical aggregates when water is gradually added into its THF solution. Upon irradiation with a linearly polarized Ar^+ laser beam, the spherical aggregates become elongated, which may be due to an increase of the chain rigidity of PCN induced by the cis−trans transition of azobenzene segments. Such an experiment carried out is not unlike the case when the value of k_a is increased in the present work. As can be seen in Figure 12, a structural transition from sphere to string can be found with an increase in k_a (increasing the rigidity of the A-block).

We would like to clarify that coil−coil copolymers as well as rod−coil copolymers can form various aggregation structures in a selective solvent, as observed in experiments. However, only a limited range of structures are observed in the present simulation. In experiments, vesicle formation by AB copolymers is the most commonly observed class of aggregates with a bilayer structure. The formation of vesicles containing a rigid building block is a challenging topic in computer simulation. We do not find the formation of this type of structure based on our model and simulation conditions. This result may be due to the initial structure employed in our simulations, where we initially set the copolymers with a regular BCC packing lamellar mode. Changes in the direction of copolymer molecules in these aggregates hardly ever occur except at the edge of the aggregates. We can only see changes in the shape viewing from the direction of molecular axes and changes in aggregation number. Further simulations on the formation of vesicles are still undergoing.

On the other hand, it should be noted that the differences in concentration and shape (chemical structure) of copolymer can affect the packing manner of the segments of copolymers, which further affect the aggregation structures. Meanwhile, changing the composition of the copolymers can also play some role in the formation of different aggregation structures. Figure 13 shows the influence of the block length on the micellization behavior. Figure 13a shows the phase diagram plotted in B-block length vs ε_{AA} at a fixed A-bead number of 8 with $f_R = 0.71$. With increasing B-block length, the region of small aggregates becomes wider, and the onsets of string and disk formation move to higher ε_{AA}. Figure 13b shows the phase diagram plotted in A-block length vs ε_{AA} with a fixed B-bead number of 9. Three different A-bead numbers of 8, 10, and 12 are presented, where f_R values are about 0.57, 0.55, and 0.55, respectively. It is clearly seen that at a similar rigid fraction, with increasing the core-forming A-block length, the onsets of string and disk formation move to lower ε_{AA}. The region of small aggregates becomes narrower. As can be also observed in Figure 13b, unlike the influence of the B-block length, the CMI is dramatically decreased with an increase in the A-block length.

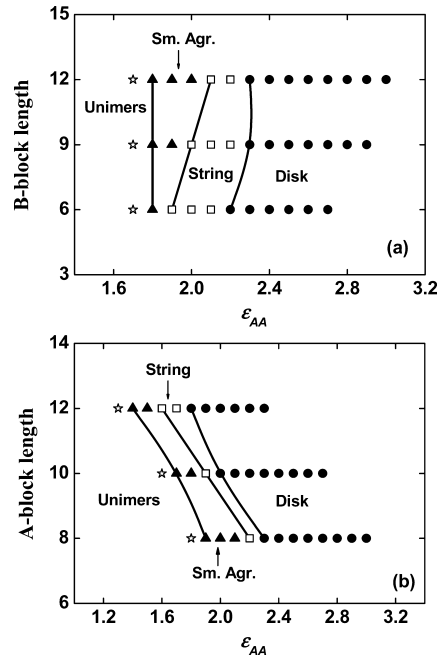

Figure 13. Simulation phase diagrams for diblock copolymers plotted in block lengths vs ε_{AA}: (a) B-block length vs ε_{AA} and (b) A-block length vs ε_{AA}. Regions of disk (●), string (□), small aggregate (▲), and unimer (☆) are shown.

We also present the effect of concentration on the phase behavior (see Supporting Information). Changing cell size and copolymer numbers will vary the copolymer concentration. It is found that with decreasing the cell size and (or) increasing the copolymer numbers, which results in the increase of concentration, a slight increase of CMI can be found. However, there is only a negligible change of the onsets of string and disk formation. It should be kept in mind that this simulation describes low copolymer concentrations. At higher concentrations, more aggregation structures may be observed because the interaction between micelles may become important. These types of interactions are outside the scope of the present study.

In this simulation, an important point to bear in mind is that the simulated block copolymer only consists of several beads. This artificially can increase the importance of fluctuations relative to really long copolymers. Unlike the small molecule systems, long entangled chains have to move in specific ways, which are limited by the fact that they are connected to other chains and they cannot cut through each other.[56] Such a situation can play some role in the aggregation dynamics. The entanglement of chains may affect the packing manner of core-forming blocks as well as corona-forming blocks, which may further result in various aggregation structures. However, it is not possible to perform simulations for the time and distance scales considered here for models containing long entangled copolymers. In this article, we just want to show an insight of influence of chain conformation transition on the aggregation behavior. It is explicitly shown that, based on our model, the aggregation structures and structure transitions can be modulated by tailoring the chain conformation. The simulation result may carry out a primary sense of micellization behavior between coil−coil copolymers and rod−coil copolymers. On the other hand, stimuli-responsive copolymeric aggregates have received much attention because of their sensitivity to the environment, which can be stimulated by pH, temperature, light, and so on.[57−59]

Some supramolecular organizations of the copolymers can be tuned by stimulating conformational changes in the hydrophobic or (and) the hydrophilic block. In the current simulation, we investigated the self-assembly behavior of diblock copolymers containing a chain-conformation changeable core-forming block, and the concomitant changes in the micelle structures may be used to manipulate their properties.

Conclusions

A Brownian dynamics is used to simulate the influence of chain conformation of core-forming A-block changing from rigid to flexible on self-assembly behavior of AB diblock copolymers. Because of the tendency of orientational packing of A-blocks with a high rigid fraction, a disk structure can be formed at a strong aggregation interaction between A-bead pairs. Transitions of aggregation structure from disk to string, further to small aggregates, and to unimers are observed with decreasing interaction. With a decrease in the rigid fraction of the A-block, the regions of these morphologies are shifted, and a spherical structure with a random packing of the A-blocks within the core appears. The phase diagrams for the influences of the rigid potion location within the A-block and the chain rigidity of the A-block are also constructed. It is found that even at a fixed rigid fraction, the variation in the rigid portion location can change the aggregation structure and modify the phase diagram. The tendency of aggregation structure transitions induced by decreasing the chain rigidity of A-block is similar to that by decreasing the rigid fraction of A-block. Some simulation results are in agreement with the existing experimental observations.

Acknowledgment. This work was supported by the National Natural Science Foundation of China (50673026) and by the Shanghai Chenguang Project (2007CG38). Support from Projects of Shanghai Municipality (09XD1401400, 0952 nm05100, 082231, and B502) is also appreciated.

Supporting Information Available: Influence of copolymer concentration on phase behavior. This material is available free of charge via the Internet at http://pubs.acs.org.

References and Notes

(1) Jenekhe, S. A.; Chen, X. L. *Science* **1998**, *279*, 1903–1906.
(2) Jenekhe, S. A.; Chen, X. L. *Science* **1999**, *283*, 372–375.
(3) Chen, J. T.; Thomas, E. L.; Ober, C. K.; Mao, G. P. *Science* **1994**, *273*, 343–346.
(4) Stupp, S. I.; LeBonheur, V.; Walker, K.; Li, L. S.; Huggins, K. E.; Keser, M.; Amstutz, A. *Science* **1997**, *276*, 384–389.
(5) Lee, M.; Cho, B. K.; Zin, W. C. *Chem. Rev.* **2001**, *101*, 3859–3892.
(6) Wang, X. S.; Guerin, G.; Wang, H.; Wang, Y. S.; Manners, I.; Winnik, M. A. *Science* **2007**, *317*, 644–647.
(7) Chochos, C. L.; Tsolakis, P. K.; Gregoriou, V. G.; Kallitsis, J. K. *Macromolecules* **2004**, *37*, 2502–2510.
(8) Zhang, L.; Eisenberg, A. *Science* **1995**, *268*, 1728–1731.
(9) Zhang, L.; Yu, K.; Eisenberg, A. *Science* **1996**, *272*, 1777–1779.
(10) Riess, G. *Prog. Polym. Sci.* **2003**, *28*, 1107–1170.
(11) Klok, H. A.; Lecommandoux, S. *Adv. Mater.* **2001**, *13*, 1217–1229.
(12) Blanazs, A.; Armes, S. P.; Ryan, A. J. *Macromol. Rapid Commun.* **2009**, *30*, 267–277.
(13) Linse, P. In *Amphiphilic Block Copolymers: Self-Assembly and Applications*; Alexandridis, P., Lindman, B., Eds.; Elsevier: Amsterdam, 2000.
(14) Leiber, L.; Orland, H.; Wheeler, J. C. *J. Chem. Phys.* **1983**, *79*, 3550–3557.
(15) Borisov, O. V.; Zhulina, E. B. *Macromolecules* **2003**, *36*, 10029–10036.
(16) Halperin, A. *Macromolecules* **1990**, *23*, 2724–2731.
(17) Semenov, A. N. *Mol. Cryst. Liq. Cryst.* **1991**, *209*, 191–196.
(18) Williams, D. R. M.; Fredrickson, G. H. *Macromolecules* **1992**, *25*, 3561–3568.
(19) Muller, M.; Schick, M. *Macromolecules* **1996**, *29*, 8900–8903.
(20) Lin, J.; Lin, S.; Zhang, L.; Nose, T. *J. Chem. Phys.* **2009**, *130*, 094907–1-7.
(21) Lin, J.; Lin, S.; Liu, P.; Hiejima, T.; Furuya, H.; Abe, A. *Macromolecules* **2003**, *36*, 6267–6272.
(22) Teramoto, A. *Prog. Polym. Sci.* **2001**, *26*, 667–720.
(23) Zimm, B. H.; Bragg, J. K. *J. Chem. Phys.* **1959**, *31*, 526–535.
(24) Muroga, Y. *Biopolymer* **2000**, *54*, 58–63.
(25) Abe, A.; Ballauff, M. In *Liquid Crystallinity in Polymers*; Ciferri, A., Ed.; VCH Publishers: New York, 1991.
(26) Babin, J.; Rodriguea-Hernandez, J.; Lecommandoux, S.; Klok, H. A.; Achard, M. F. *Faraday Discuss.* **2005**, *128*, 179–192.
(27) Ding, W.; Lin, S.; Lin, J.; Zhang, L. *J. Phys. Chem. B* **2008**, *112*, 776–783.
(28) Allen, M. P.; Tildesley, D. J. *Computer Simulation of Liquids*; Oxford University Press: New York, 1987.
(29) Viduna, D.; Milchev, A.; Binder, K. *Macromol. Theory Simul.* **1998**, *7*, 649–658.
(30) Milchev, A.; Bhattacharya, A.; Binder, K. *Macromolecules* **2001**, *34*, 1881–1893.
(31) Yu, B.; Li, B. H.; Sun, P. C.; Chen, T. H.; Jin, Q. H.; Ding, D. T.; Shi, A. C. *J. Chem. Phys.* **2005**, *123*, 234902−1–8.
(32) Capone, B.; Pierleoni, C.; Hansen, J. P.; Krakoviack, V. *J. Phys. Chem. B* **2009**, *113*, 3629–3638.
(33) Pierleoni, C.; Addison, C.; Hansen, J. P.; Krakoviack, V. *Phys. Rev. Lett.* **2006**, *96*, 128302−1–4.
(34) Murat, M.; Grest, G. S.; Kremer, K. *Macromolecules* **1999**, *32*, 595–609.
(35) Alsunaidi, A.; Abu-Sharkh, B. F. A. *J. Chem. Phys.* **2003**, *119*, 9894–9902.
(36) Schultz, A. J.; Hall, G. K.; Genzer, J. *Macromolecules* **2005**, *38*, 3007–3016.
(37) Chushak, Y.; Travesset, A. *J. Chem. Phys.* **2005**, *123*, 234905−1–7.
(38) Tsige, M.; Mattsson, T. R.; Grest, G. S. *Macromolecules* **2004**, *37*, 9132–9138.
(39) Srinivas, G.; Pitera, J. W. *Nano Lett.* **2008**, *8*, 611–618.
(40) (a) Groot, R. D.; Madden, T. J. *J. Chem. Phys.* **1998**, *108*, 8713–8724. (b) Groot, R. D.; Madden, T. J.; Tildesley, D. J. *J. Chem. Phys.* **1999**, *108*, 9737–9749.
(41) Qian, H. J.; Lu, Z. Y.; Chen, L. J.; Li, Z. S.; Sun, C. C. *Macromolecules* **2005**, *38*, 1395–1401.
(42) Huang, C. I.; Hsueh, H. Y.; Lan, Y. K.; Lin, Y. C. *Macromol. Theory Simul.* **2007**, *16*, 77–85.
(43) Zhang, Z. L.; Horsch, M. A.; Lamm, M. H.; Glotzer, S. C. *Nano Lett.* **2003**, *10*, 1341–1346.
(44) Horsch, M. A.; Zhang, Z. L.; Glotzer, S. C. *Phys. Rev. Lett.* **2005**, *95*, 056105−1–4.
(45) Horsch, M. A.; Zhang, Z. L.; Glotzer, S. C. *J. Chem. Phys.* **2006**, *125*, 184903−1–12.
(46) Lin, S.; Numasawa, N.; Nose, T.; Lin, J. *Macromolecules* **2007**, *40*, 1684–1692.
(47) Cui, J.; Zhu, J.; Ma, Z.; Jiang, W. *Chem. Phys.* **2006**, *321*, 1–9.
(48) Song, J.; Shi, T.; Li, Y.; Chen, J.; An, L. *J. Chem. Phys.* **2008**, *129*, 054906.
(49) OCTA Home Page. http://octa.jp (accessed Jan 8, 2007).
(50) Lin, S.; Numasawa, N.; Nose, T.; Lin, J. *Mol. Cryst. Liq. Cryst.* **2007**, *466*, 53–76.
(51) Bourov, G. K.; Bhattacharya, A. *J. Chem. Phys.* **2003**, *119*, 9219–9225.
(52) Bourov, G. K.; Bhattacharya, A. *J. Chem. Phys.* **2005**, *122*, 044702−1–6.
(53) Grest, G. S.; Kremer, K. *Phys. Rev. A* **1986**, *33*, 3628–3631.
(54) Grest, G. S.; Lacasse, M. D. *J. Chem. Phys.* **1996**, *105*, 10583–10594.
(55) Wang, D. R.; Ye, G.; Wang, X. G. *Macromol. Rapid Commun.* **2007**, *28*, 2237–2243.
(56) Kremer, K.; Grest, G. S. *J. Chem. Phys.* **1990**, *92*, 5057–5086.
(57) Li, M. H.; Keller, P. *Soft Matter* **2009**, *5*, 927–937.
(58) Zhao, Y. *Chem. Rec.* **2007**, *7*, 286–294.
(59) Raez, J.; Tomba, J. P.; Manners, I.; Winnik, M. A. *J. Am. Chem. Soc.* **2003**, *125*, 9546–9547.

JP904707A